Supporting Information for

Aggregation-induced emission enhancement (AIEE) of tetrarhenium(I) metallacycles and their application as luminescent sensors for nitroaromatics and antibiotics

Mohammad Nurnabi,[a] Shunmugasundaram Gurusamy,[b] Jing-Yun Wu,[c] Chung-Chou Lee,[a] Malaichamy Sathiyendiran,[a] Sheng-Ming Huang,[a] Che-Hao Chang,[a] Ito Chao,[a] Gene-Hsiang Lee,[d] Shie-Ming Peng,[d] Veerasamy Sathish,[e] Pounraj Thanasekaran,*[,f] and Kuang-Lieh Lu*[,a,g]

[a]*Institute of Chemistry, Academia Sinica, Taipei 115, Taiwan*
[b]*PG and Research Department of Chemistry, V. O. Chidambaram College, Tuticorin – 628 008, Tamil Nadu, India*
[c]*Department of Applied Chemistry, National Chi Nan University, Nantou 545, Taiwan*
[d]*Department of Chemistry, National Taiwan University, Taipei 107, Taiwan*
[e]*Department of Chemistry, Bannari Amman Institute of Technology, Sathyamangalam – 638 401, India*
[,f]*Department of Chemistry, Pondicherry University, Puducherry 605 014, India*
[g]*Department of Chemistry, Fu Jen Catholic University, New Taipei City 242, Taiwan*

*To whom correspondence should be addressed.
E-mail: ptsekaran.chem@pondiuni.edu.in (P. Thanasekaran)
E-mail: kllu@gate.sinica.edu.tw (K.-L. Lu)

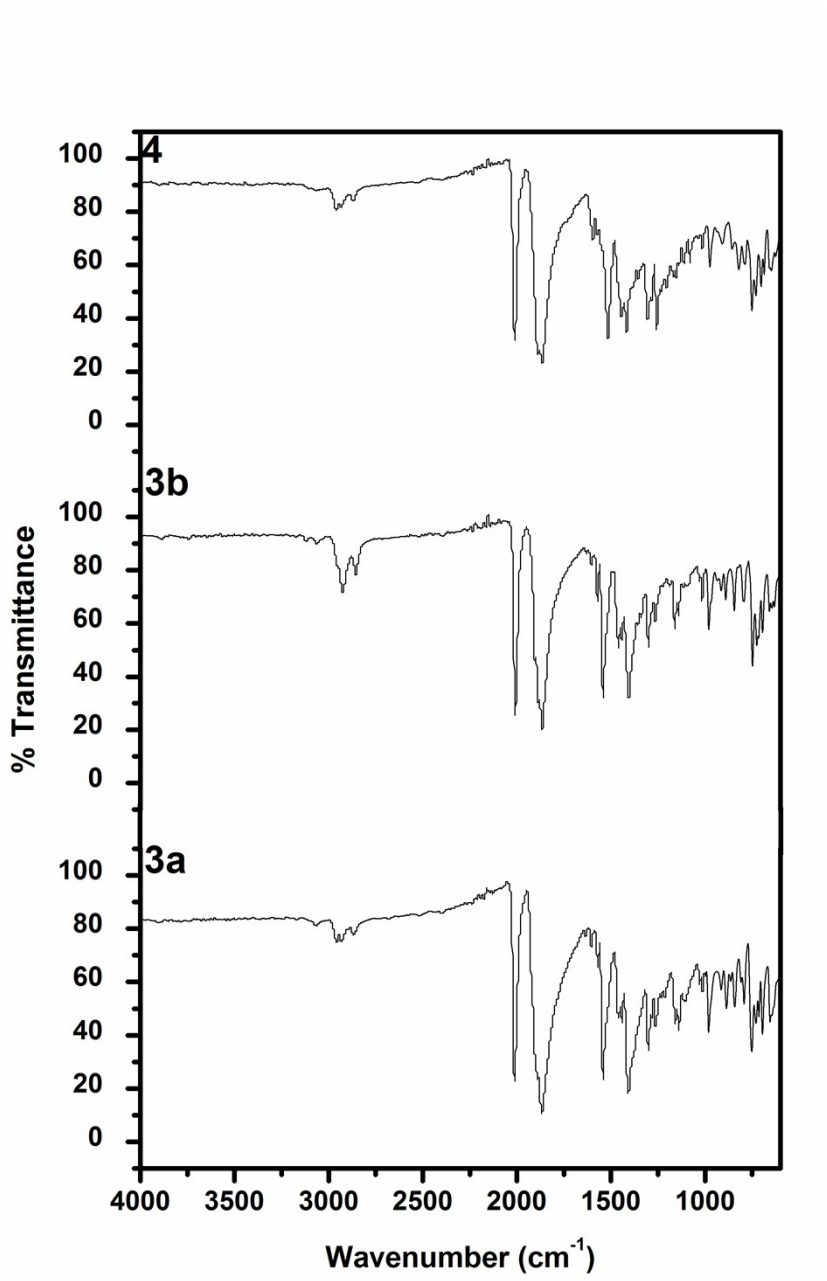

Figure S1. ATR-IR spectra of compounds **3a**, **3b** and **4**.

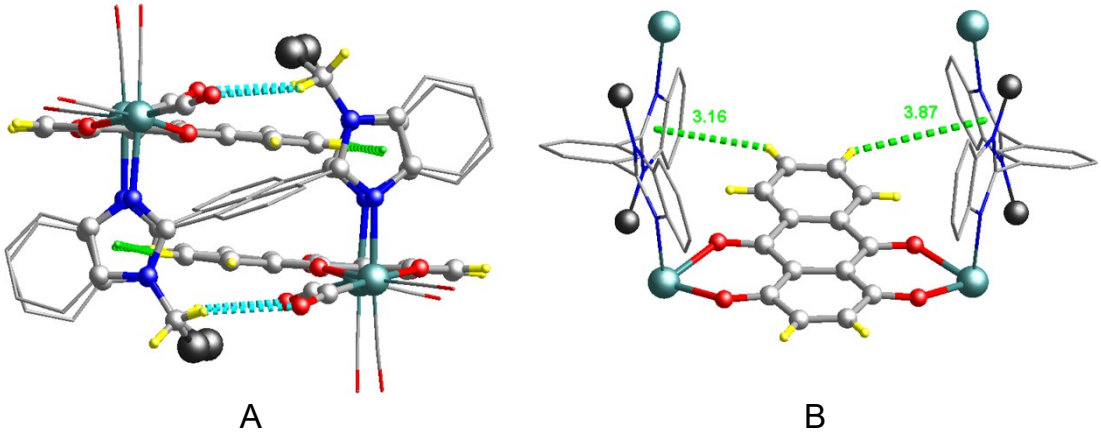

Figure S2. (A) Side view of the molecular structure of **3a**, showing potential C–H···π (green dashed lines) and C–H···O≡C (cyan dashed lines) interactions. Color scheme: teal, Re; red, O; blue, N; gray, C; yellow, H; dark gray, C_3H_7 group. (B) Highlight of potential C–H···π (green dashed lines) interactions in **3a** Color scheme: teal, Re; red, O; blue, N; gray, C; yellow, H; dark gray, C_4H_9 groups.

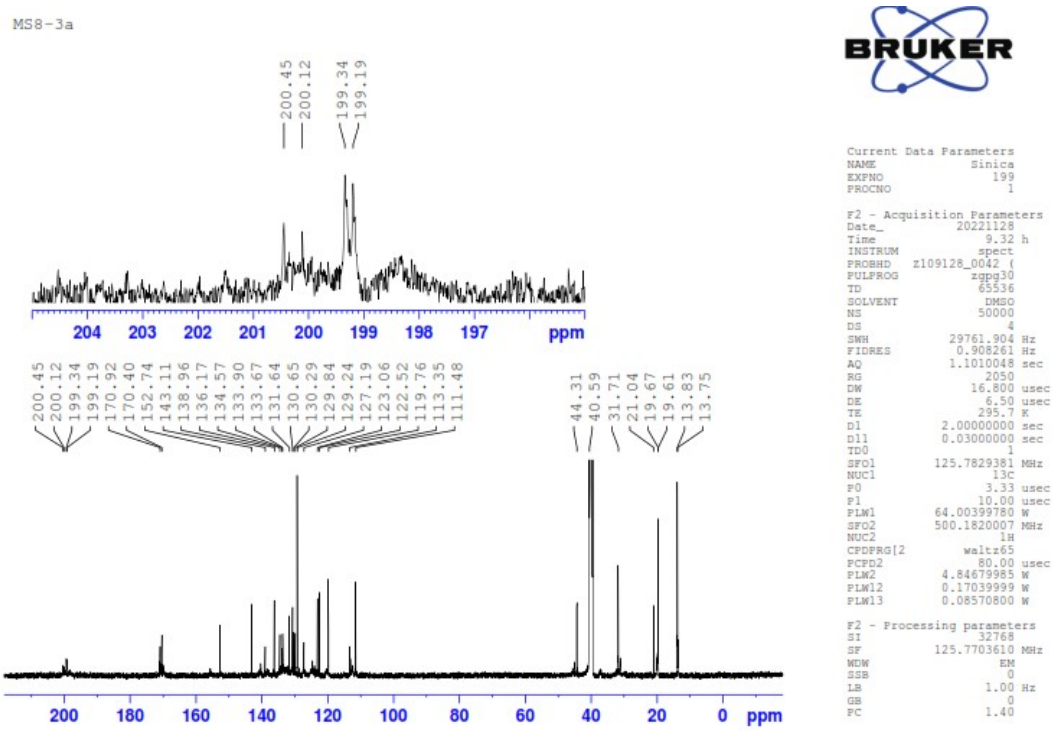

Figure S3. ^{13}C NMR spectrum of compound **3a**.

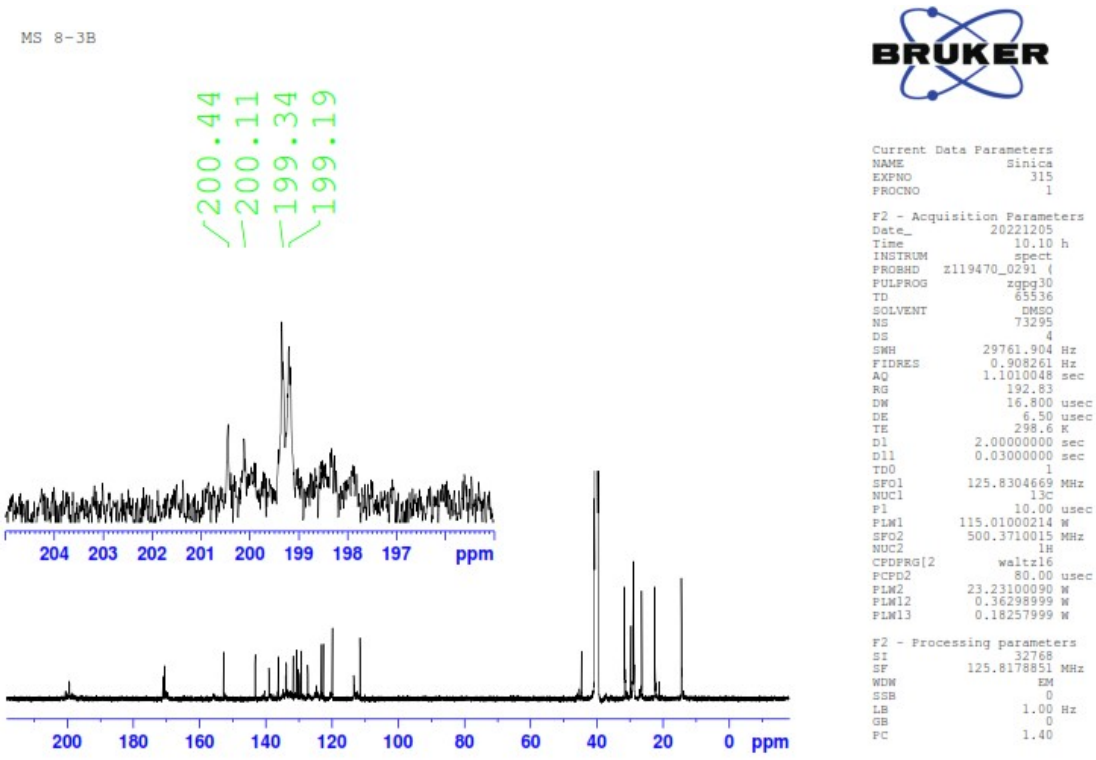

Figure S4. ^{13}C NMR spectrum of compound **3b.**

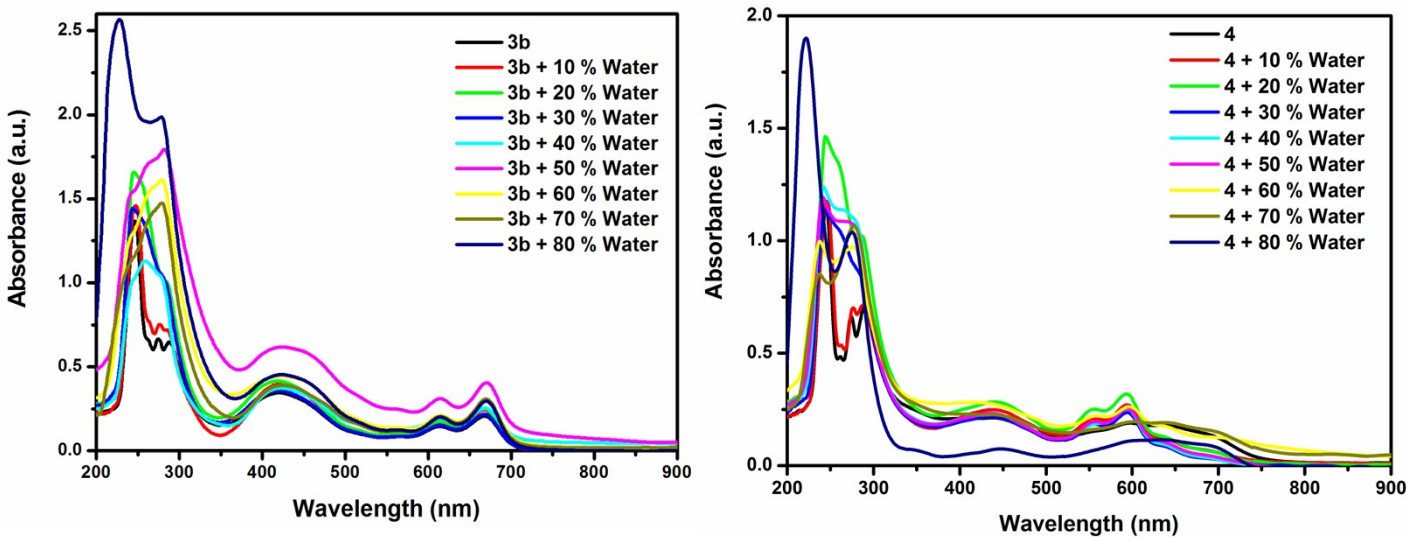

Figure S5. UV–visible spectral changes for compounds **3b** and **4** (10 μM) upon the addition of various water content (0–90%) in H_2O:THF mixture.

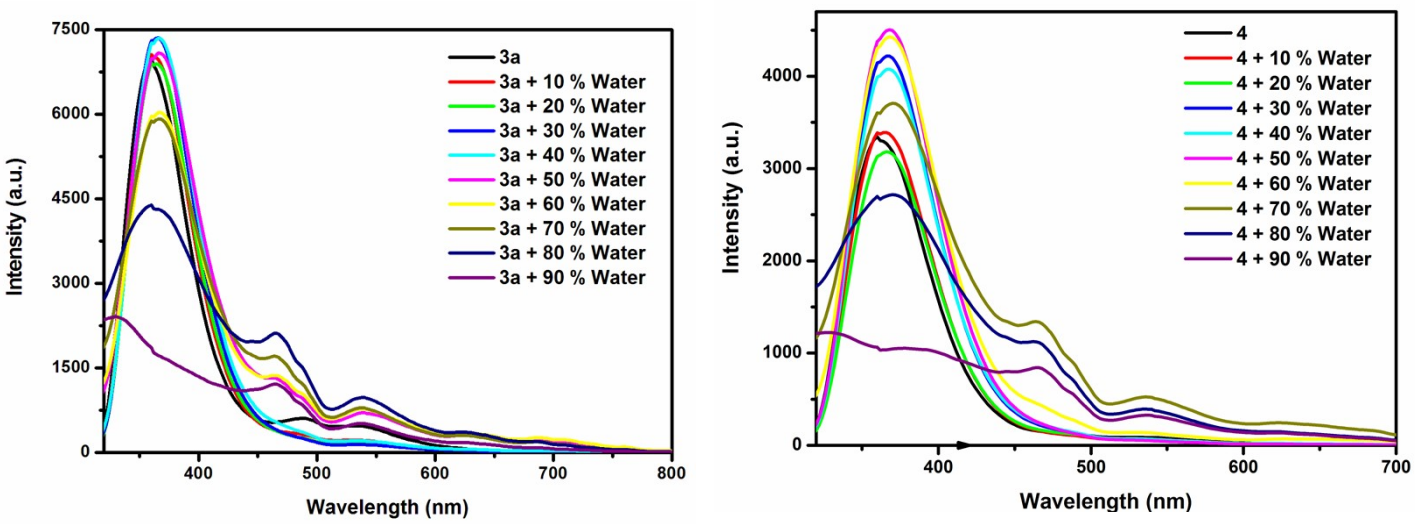

Figure S6. Changes in the fluorescence spectra of **3a** and **4** (10 μM) upon the addition of water (10–90%) to a H_2O:THF mixture (λ_{ex} = 320 nm)

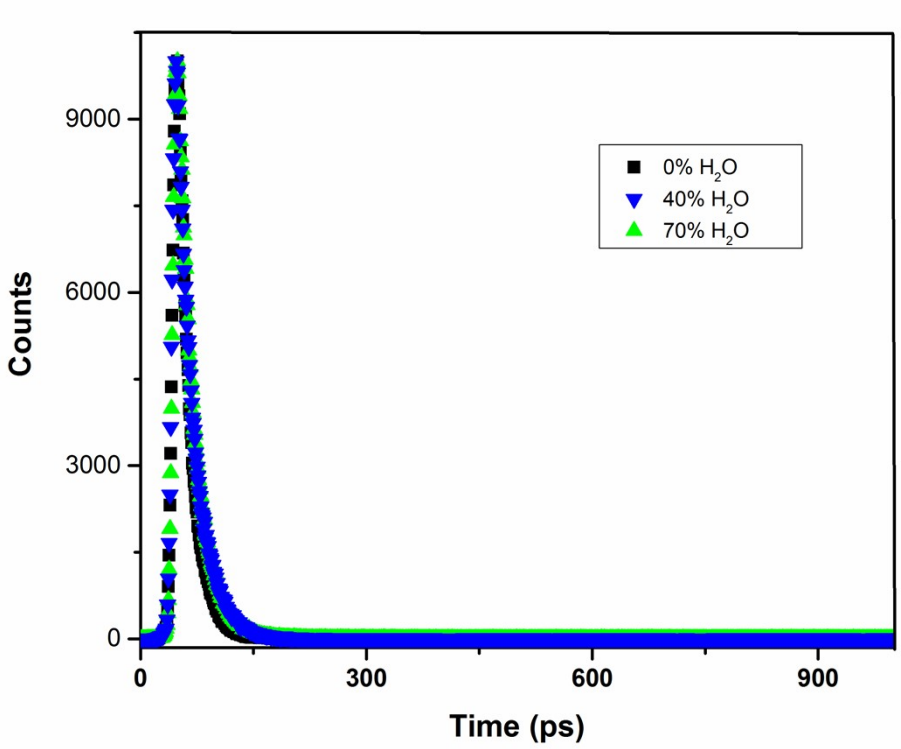

Figure S7. Life-time decay profile of compound **3b** in the presence of different water contents (0, 40 & 70%) in THF.

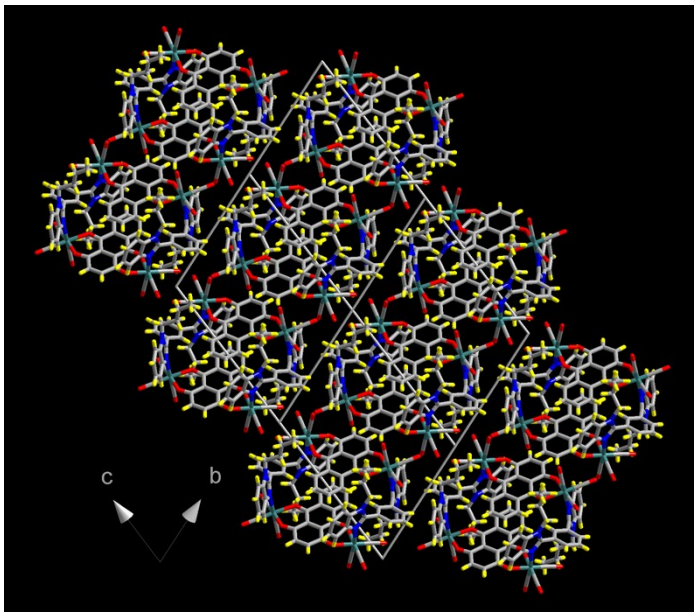

Figure S8. Crystal packing diagram of **3a** viewed along the crystallographic *a*-axis.

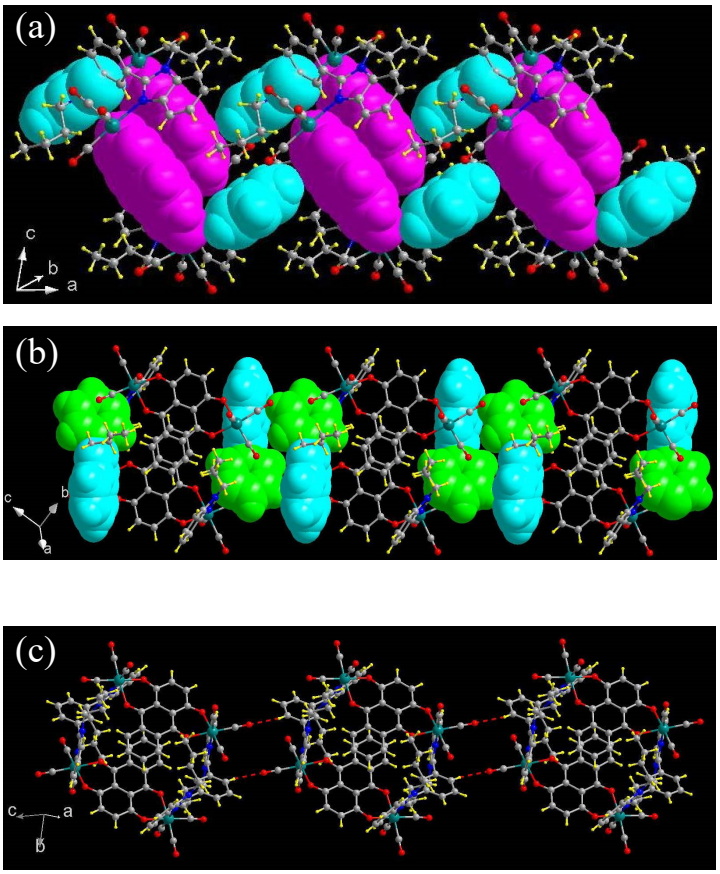

Figure S9. (a) Highlights of the column-stacking of the tetrarhenium compound **3a** along the crystallographic *a*-axis, assisted by C–H···π interactions between the phenyl ring of the benzimidazolyl moiety of **1a** (cyan-colored space-filling model) and the dhaq ligand (pink-colored space-filling model). (b) Highlights the C–H···π interactions between the central benzene ring and the benzimidazolyl moiety of **1a** (cya) in neighboring molecules of **3a**. (c)

The C–H···O≡C hydrogen bonds between the central benzene ring of **1a** in a molecule and the carbonyl groups of neighboring molecules.

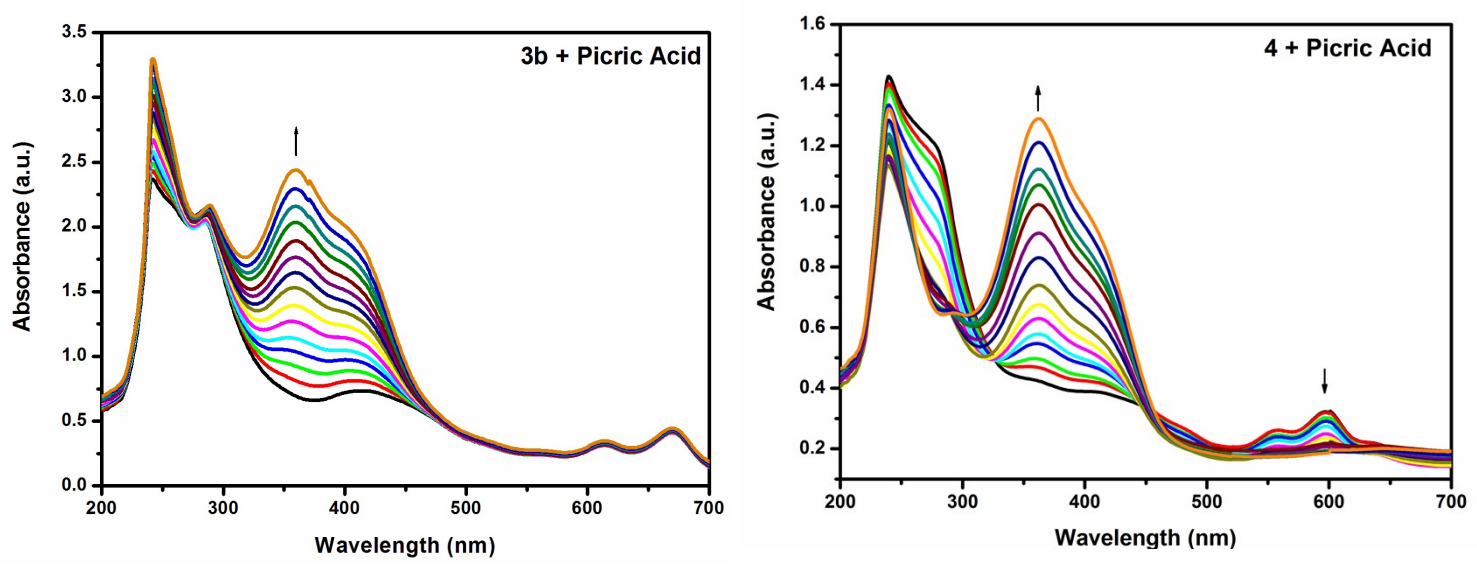

Figure S10. Changes in the absorption spectra of **3b** and **4** (10 μM) upon the addition of PA (0-15 μM) in 50:50 H_2O:THF mixture.

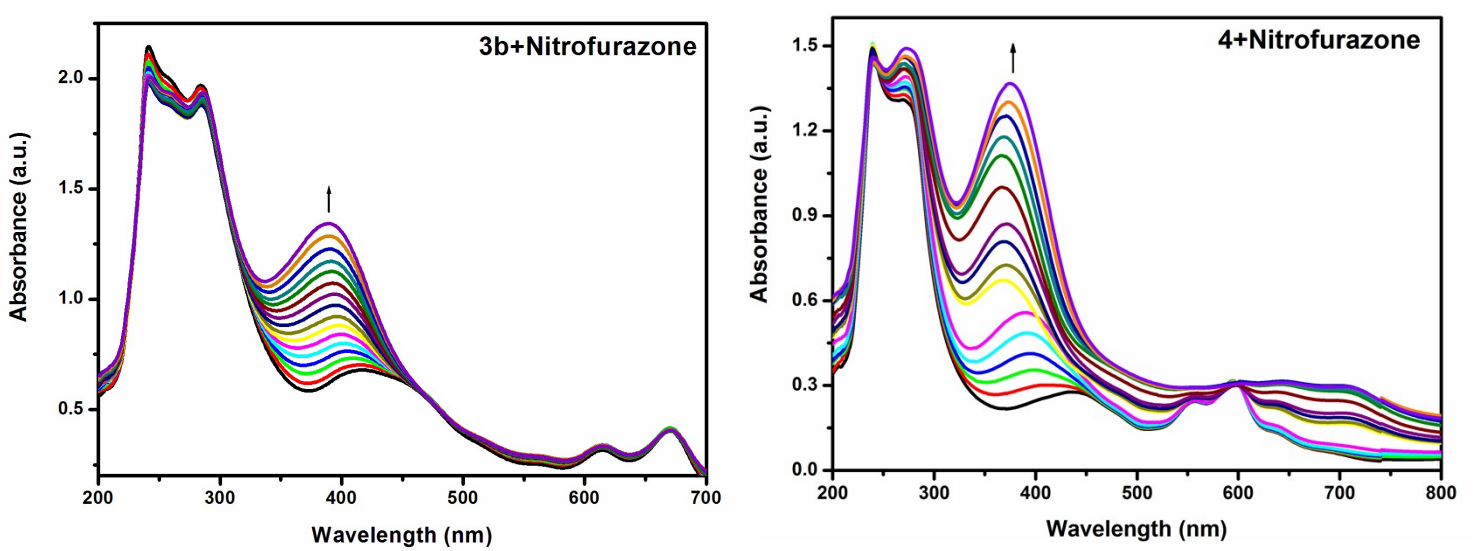

Figure S11. Changes in the absorption spectra of **3b** and **4** (10 μM) upon the addition of nitrofurazone (0–15 μM) to a 50:50 H_2O:THF mixture.

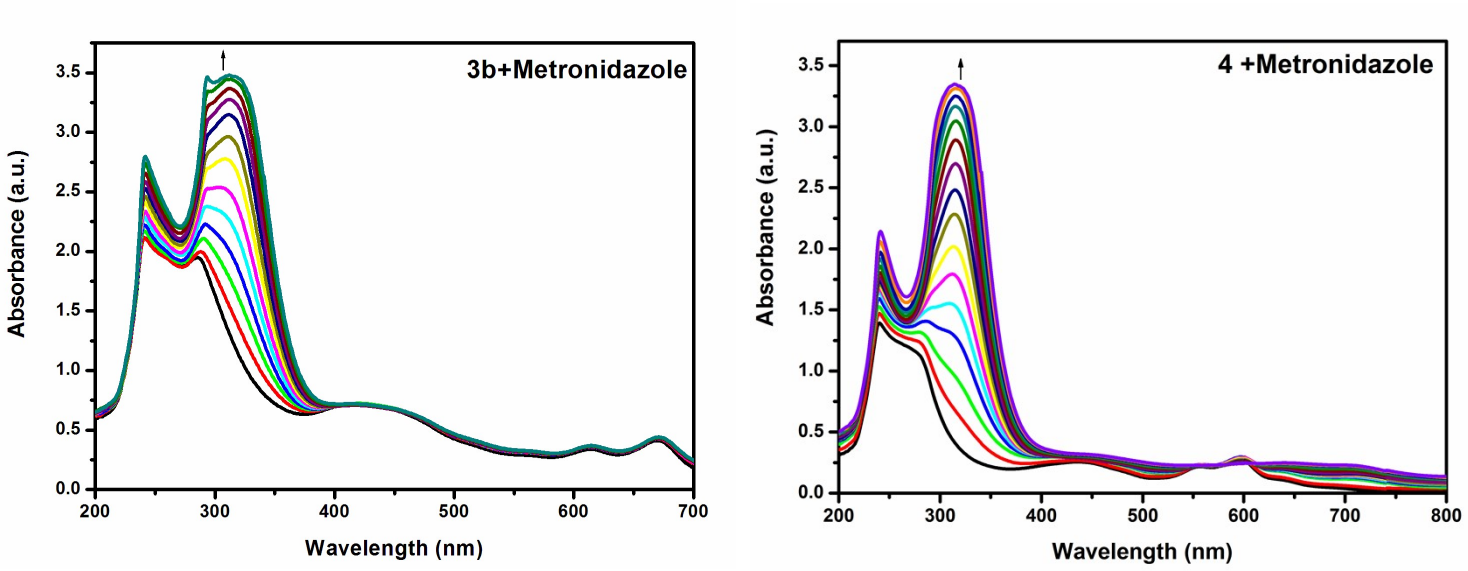

Figure S12. Changes in the absorption spectra of **3b** and **4** (10 μM) upon the addition of metronidazole (0–15 μM) to a 50:50 H_2O:THF mixture.

Table S1. Crystallographic Data of **3a** and **4**·3C_7H_8

	3a	**4**·3C_7H_8
formula	$C_{96}H_{72}N_8O_{20}Re_4$	$C_{117}H_{96}N_8O_{22}Re_4$
M_r	2402.42	2710.82
crystal system	triclinic	monoclinic
space group	$P\bar{1}$	$P2_1/n$
a (Å)	11.5803 (8)	15.7647 (9)
b (Å)	13.1966 (8)	14.9159 (8)
c (Å)	16.1427 (11)	22.4345 (13)
α (deg)	67.950 (2)	90
β (deg)	79.118 (2)	90.631 (1)
γ (deg)	70.650 (2)	90
V (Å^3)	2151.5 (2)	5275.0 (5)
Z	1	2
T (K)	296(2)	150 (2)
λ (Å)	0.71073	0.71073
D_{calc} (g/cm^3)	1.854	1.707
μ (mm^{-1})	5.687	4.651
F(000)	1164	2660
goodness-of-fit	1.042	1.201
R1[a]/wR2[b] [$I > 2\sigma(I)$]	0.0333/0.0800	0.0840/0.1780
R1[a]/wR2[b] (all data)	0.0503/0.0874	0.0968/0.1855
largest residuals (e Å^{-3})	1.017/–1.982	6.361/–3.663

[a] $R_1 = \sum \big||F_o| - |F_c|\big| \Big/ \sum |F_o|$. [b] $wR_2 = \{\sum [w(F_o^2 - F_c^2)^2] \Big/ \sum [w(F_o^2)^2]\}^{1/2}$

Table S2. Stern-Volmer quenching constant values (K_{sv}, M^{-1}) for the reaction of metallacycles **3b** and **4** by PA and antibiotics.

Compounds	Nitroaromatics & Antibiotics	SV Quenching constant
		K_{sv} (M^{-1})
3b	Picric acid	2.6591×10^4
3b	Metronidazole	3.8889×10^4
3b	Nitrofurazone	5.9368×10^4
4	Picric acid	4.3853×10^4
4	Metronidazole	2.6643×10^4
4	Nitrofurazone	3.1772×10^4